Inorganic Chemistry

Article

pubs.acs.org/IC

Metal–Organic Frameworks as Hosts for Photochromic Guest Molecules

D. Hermann,[†] H. Emerich,[‡] R. Lepski,[§] D. Schaniel,[∥,⊥] and U. Ruschewitz*,[†]

[†]Department of Chemistry, University of Cologne, Greinstr. 6, 50939 Cologne, Germany

[‡]SBNL at the European Synchrotron Radiation Facility, BP 220, 6 rue Horowitz, F-38043 Grenoble, France

[§]Physics I, University of Cologne, Zülpicher Str. 77, 50939 Cologne, Germany

[∥]Université de Lorraine, CRM2, UMR 7036, Vandoeuvre-les-Nancy, F-54506, France

[⊥]CNRS, CRM2, UMR 7036, Vandoeuvre-les-Nancy, F-54506, France

Supporting Information

ABSTRACT: Several metal–organic framework compounds (MOF-5, MIL-68(Ga), MIL-68(In), MIL-53(Al)) were loaded with azobenzene (AZB), as confirmed by XRPD measurements and elemental analysis. By IR spectroscopy, it was shown that the light-induced *trans*/*cis* isomerization of AZB in these hybrid host–guest compounds is improved compared to that of solid AZB. A population of the excited *cis* state up to 30% has been obtained for $AZB_{0.66}$@MIL-68(In). However, no light-induced *trans*/*cis* isomerization was observed for $AZB_{0.5}$@MIL-53(Al). Structural models obtained from high-resolution synchrotron powder diffraction data show that AZB molecules are densely packed within the channels of MIL-53(Al) so that no *trans*/*cis* isomerization can occur. A different situation was observed for AZB in the larger channels of MIL-68(Ga). Thus, this investigation shows the influence of the host material on the switching behavior of the embedded AZB molecules.

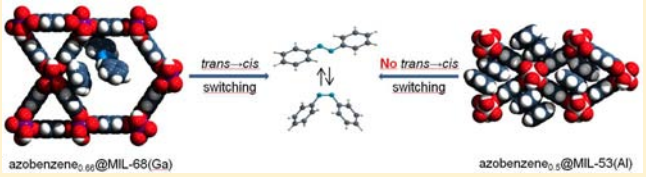

INTRODUCTION

Metal–organic frameworks (MOFs) are a class of inorganic–organic hybrid materials that combine a crystalline nature with an ordered pore structure.[1] This field is widely explored with respect to gas adsorption,[2,3] the separation of gases[4,5] and liquids,[5−7] and heterogeneous catalysis.[8] To explain the selectivities in the adsorption of ethylbenzene, *ortho*-, *meta*-, and *para*-xylenes, the crystal structures of loaded MIL-47(V) were solved from X-ray powder diffraction data, indicating that a different packing of the isomers is responsible for their differing adsorption behavior.[5] However, the embedment of larger functional molecules is less investigated up to now. Several publications are concerned with the inclusion of precursor molecules in MOFs to obtain metal nanoparticles inside the MOF framework through decomposition of the guest molecules.[9,10] Férey et al. investigated MOFs as hosts for drug molecule encapsulation.[11,12] In a different approach, we have started a while ago to incorporate photoswitchable complexes[13] and azo dyes[14] into different MOFs to obtain new materials with interesting optical properties. Because of its well-known photochromic behavior, that is, well-separated absorption bands in the UV/vis spectrum for the *trans* and *cis* isomers,[15] azobenzene (AZB) can act as a molecular switch, when illuminated with light. This process is well-studied in solution.[16] For porous coordination polymers (MOFs), it was found that switching of azo groups, covalently bound to linker molecules as a side chain, is possible,[17−20] whereas when incorporated in the MOF backbone, switching of azo groups could not be achieved up to now.[21,22] Azobenzene molecules weakly bound via van der Waals interactions to the host have already been incorporated in zeolites (ZSM-5) and aluminophosphates, where the lifetime of the metastable *cis* isomer was found to depend on the chosen host matrix,[23] in zinc saccharate, a 3D coordination network,[24] and in the flexible porous coordination polymer $[Zn_2(terephthalate)_2(triethylenediamine)]_n$.[25] Most remarkably, in the latter example, it was shown that switching of AZB leads to a reversible structural transformation of the flexible coordination polymer and thus to drastic changes in the gas adsorption properties. We have already briefly reported our results on the successful *trans*/*cis* isomerization of AZB incorporated in MOF-5.[14] In this work, we will present our investigations on further AZB@MOF hybrid materials and additionally the crystal structures of MOFs with embedded photochromic guest molecules, an essential knowledge for an understanding of the different optical properties obtained for the investigated materials.

EXPERIMENTAL SECTION

X-ray Powder Diffraction. Laboratory measurements were carried out on a STOE Stadi P diffractometer (Ge monochromator, PSD detector) with Cu–Kα_1 radiation, a step size of 0.01°, and a measurement time of 5 s/step. For each diffraction pattern, four measurements were added.

Received: December 28, 2012
Published: February 14, 2013

   dx.doi.org/10.1021/ic302856b | *Inorg. Chem.* 2013, 52, 2744−2749

Synchrotron Powder Diffraction. High-resolution synchrotron measurements of AZB_5@MOF-5 (**1**) were performed with a NaI scintillation detector at the beamline BL9 of DELTA, TU Dortmund, at 298 K with a wavelength of 0.815765 Å and a step size of 0.004°. The measurement time was 4 s/step.

High-resolution synchrotron powder diffraction data of $AZB_{0.66}$@MIL-68(In) (**2**), $AZB_{0.66}$@MIL-68(Ga) (**3**), and $AZB_{0.5}$@MIL-53(Al) (**4**) were collected at the Swiss Norwegian BeamLine (SNBL BM01B) at ESRF. The wavelength was calibrated with a Si standard NIST 640c to 0.50195 Å. The diffractometer is equipped with six counting channels, delivering six complete patterns collected simultaneously with a small 1.1° offset in 2θ. A Si(111) analyzer crystal is mounted in front of each NaI scintillator/photomultiplier detector. Data were collected at 298 and 120 K (cryostreamer with cold N_2) between 0.5 and 30.0° in 2θ with steps of 0.002° and 300−500 ms integration time per data point. For each sample, several patterns were collected and summed up for the final pattern. The data collection time for each sample was 2−3 h (298 K) and 6−13 h (120 K).

All synchrotron powder experiments were carried out in sealed glass capillaries of 0.7−1.0 mm in diameter (Hilgenberg).

Structure Solution and Refinement. The obtained diffraction patterns were indexed with the programs ITO[26] and FOX.[27] Le Bail fits in Jana2006[28] were used to refine the unit cells, zero shifts, and profile parameters. For the structure solution, the atomic positions of MIL-53(Al)·0.7H_2bdc[29]/MIL-68(Ga)[30] were taken as starting parameters of the host together with the refined unit cell parameters. Furthermore, the molecular structure of azobenzene[31] was used on the starting position 0 0 0 in FOX. The global optimization algorithm was run in the parallel tempering mode and converged after approximately 80 000 trials for $AZB_{0.5}$@MIL-53(Al) (R values: R_p = 0.1608 and wR_p = 0.2057). The occupancy of AZB was refined in the structure solution process. For the structure solution of $AZB_{0.66}$@MIL-68(Ga), two symmetry-independent AZB molecules were placed in the unit cell, and the occupancy was set to 0.25 for both and fixed in the structure solution process. Convergence was achieved after approximately 300 000 trials with R values of R_p = 0.1719 and wR_p = 0.1750.

The Rietveld refinement of the obtained structure models was performed with GSAS.[32] To get a stable refinement, the azobenzene molecules, as well as the benzenedicarboxylate anions, were fixed with soft constraints (bond lengths, angles, and planes according to the literature values). The isotropic displacement parameters of the guest molecule atoms and the host atoms were coupled with constraints and refined afterward, if possible. The final stable refinement of $AZB_{0.5}$@MIL-53(Al) had a total of 135 parameters. For $AZB_{0.66}$@MIL-68(Ga), additional soft constraints for the Ga−O distance were necessary. The MOF network atom positions, unit cell, zero shift, and profile parameters were stably refined with a total of 70 parameters. The isotropic displacement parameters were fixed. The atom positions of both symmetry-independent azobenzene molecules had to be refined separately with the other parameters being fixed.

IR Spectroscopy. Extinction IR measurements were performed as KBr pellets on a Nicolet 5700 spectrometer. After recording the IR spectra of the ground state, the compounds were illuminated with 325 nm laser light to induce the *trans* → *cis* isomerization. To investigate the reconversion to *trans*-AZB, the compounds were illuminated with 442 nm laser light. The successive irradiation times for all compounds as well as the wavelengths are given in Table S1 (Supporting Information). In Figure 2 and Figures S2 and S3 of the Supporting Information, the ground state before irradiation is shown together with the measurements underlined in Table S1.

UV/vis Spectroscopy. The UV/vis spectrum of the solid compound $AZB_{0.5}$@MIL-53(Al) was measured in a transparent KBr pellet on a Varian CARY 05E spectrometer.

Elemental Analysis. Elemental analysis of carbon, hydrogen, and nitrogen was performed with a HEKAtech GmbH EuroEA 3000 Analyzer. In a glovebox, approximately 2 mg of each compound was filled into a tin cartridge.

Synthesis: MIL-68(Ga) ($GaOH(C_8O_4H_4)\cdot 0.9DMF\cdot zH_2O$) and MIL-68(In) ($InOH(C_8O_4H_4)\cdot 1.0DMF\cdot zH_2O$). MIL-68(Ga) and MIL-68(In) were synthesized according to the literature.[30] The respective metal salt and H_2bdc were mixed with 5.0 mL of DMF in a 23 mL Teflon autoclave and heated to 100 °C at 20 °C/h. After 48 h, the mixture was cooled to room temperature at 5 °C/h. The colorless powders were washed with DMF and dried in air. The removal of embedded DMF molecules was achieved by heating in air to 200 °C for 12 h. The activated samples were stored in a glovebox to prevent them from rehydration.

The syntheses described above were carried out with 207.4 mg of $Ga(NO_3)_3\cdot xH_2O$ and 100.0 mg of H_2bdc/408.2 mg of $In(NO_3)_3\cdot 5H_2O$ and 200.0 mg of H_2bdc.

MIL-53(Al) ($AlOH(C_8O_4H_4)$). The synthesis of MIL-53(Al) was carried out based on the literature procedure[33] with variations in the amount of the starting materials and the applied temperature programs.

$Al(NO_3)_3\cdot 9H_2O$ (1.95 g) and H_2bdc (432.0 mg) were mixed with 5.0 mL of H_2O in a 23 mL Teflon autoclave. The mixture was heated to 180 °C at 10 °C/h, and the temperature was held for 72 h and then cooled down to room temperature at 5 °C/h. MIL-53(Al)*as* was obtained as a colorless powder, washed with H_2O and DMSO, and dried in air. For removal of unreacted and embedded H_2bdc, the substance was heated in air for 7 days at 350 °C, followed by 3 days at 400 °C. After cooling to room temperature, MIL-53(Al)*lt* (≡ $AlOH(C_8O_4H_4)\cdot H_2O$) was obtained.

Guest@MOF Systems. To load the respective MOF with azobenzene via a gas phase reaction, the host material was placed in a Schlenk tube and activated for 1 h at 70 °C in a dynamic vacuum. Azobenzene was added, and the inhomogeneous mixture was heated at 50−60 °C in vacuum, until the colorless MOF turned homogeneously orange. The excess of azobenzene resublimated at the top of the glass vessel. To prevent the loaded powders from the additional adsorption of water or, in the case of MOF-5, decomposition by contact with air, all compounds were stored in a glovebox under argon atmosphere. For $AZB_{0.5}$@MIL-53(Al) (**4**), it was shown that AZB can be removed from the host by suspending **4** in acetone. The acetone solution turned yellow and after repeating the procedure three times and finally washing the residue with water, MIL-53(Al)*lt* (≡$AlOH(C_8O_4H_4)\cdot H_2O$) was obtained. Similar results were obtained for AZB_5@MOF-5 (**1**).

AZB_5@MOF-5 (1). The reaction was carried out following the general synthesis procedure as described above with 200.0 mg of MOF-5 (0.26 mmol) and 308.0 mg of azobenzene (1.69 mmol) in the ratio 1:6.5.

$AZB_{0.66}$@MIL-68(In) (2). The reaction was carried out with 50.0 mg of solvent-free MIL-68(In) (0.17 mmol) and 46.5 mg of azobenzene (0.26 mmol, ratio 1:1.5).

$AZB_{0.66}$@MIL-68(Ga) (3). The reaction was carried out with 50.0 mg of solvent-free MIL-68(Ga) (0.20 mmol) and 54.7 mg of azobenzene (0.30 mmol, ratio 1:1.5).

$AZB_{0.5}$@MIL-53(Al) (4). The reaction was carried out with 60.0 mg of MIL-53(Al)*lt* (0.27 mmol) and 39.4 mg of azobenzene (0.22 mmol, ratio 1:0.8).

RESULTS AND DISCUSSION

We selected colorless MOFs for our experiments to minimize the influence of the host lattice in optical investigations. Furthermore, it was checked by simple geometric considerations that AZB should fit into the pores or channels of the MOF structures. Finally, three MOFs of the MIL family (MIL: Matériaux de l'Institut Lavoisier) were chosen for our experiments, as they crystallize in crystal structures of lower symmetry (orthorhombic) so that symmetry-caused disorder is minimized, helping in the structural elucidation of AZB embedded in the MOF channels (see below). After activation of the chosen MOF hosts, AZB was embedded in MOF-5[34] ($Zn_4O(bdc)_3$, bdc^{2-} = 1,4-benzenedicarboxylate), MIL-68(In)[30] (In(OH)(bdc)), MIL-68(Ga)[30] (Ga(OH)(bdc)), and MIL-53(Al)[33] (Al(OH)(bdc)) via a gas phase process to exclude any solvent molecules from all further considerations.

dx.doi.org/10.1021/ic302856b | *Inorg. Chem.* 2013, 52, 2744−2749

The successful inclusion of the guest molecules was confirmed by XRPD measurements, elemental analysis, and UV/vis measurements. After embedment of AZB in MOF-5, MIL-68(In), and MIL-68(Ga), significant changes of the reflection intensities were observed caused by the electron density of the guest molecules inside the MOF pores. However, the diffraction angles mainly remained unchanged, indicating that the MOF lattice is still intact. For loaded AZB_5@MOF-5 (**1**) and unloaded MOF-5, this is shown in Figure 1. (For

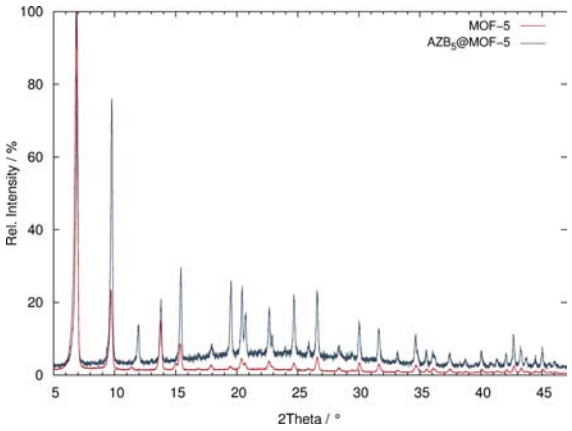

Figure 1. XRPD pattern of AZB_5@MOF-5 (blue) and unloaded MOF-5 (red) at 298 K (STOE Stadi P, Cu−Kα_1 radiation).

diffraction patterns of loaded/unloaded MIL-68(In) and MIL-68(Ga), see Figures S4 and S5 in the Supporting Information.) On the contrary, for MIL-53(Al), a flexible porous coordination polymer, a change of the reflection intensities and positions occurs (Figure S6 in the Supporting Information). Through the inclusion of AZB molecules, the framework "breathes", resulting in a deformation of the porous channels and thus the unit cell. From elemental analysis (Supporting Information, Table S2), the ratio of guest molecules per formula unit of the host material was determined: AZB_5@MOF-5 (**1**), $AZB_{0.66}$@MIL-68(In) (**2**), $AZB_{0.66}$@MIL-68(Ga) (**3**), and $AZB_{0.5}$@MIL-53(Al) (**4**). The UV/vis measurement of (**1**) showed that only the thermodynamically more stable *trans* isomer[15] was embedded in MOF-5 (Supporting Information, Figure S1), as expected from the synthesis procedure at elevated temperatures (60−80 °C).

To investigate the isomerization process of the embedded AZB molecules, the polycrystalline powders were prepared as transparent KBr pellets and illuminated with UV light (λ = 325 nm) to induce the *trans* → *cis* conversion. For $AZB_{0.66}$@MIL-68(In) (**2**) and AZB_5@MOF-5 (**1**), the reverse process was examined by irradiation with blue light (λ = 442 nm). Before and after each irradiation, IR spectra were collected (Figure 2; for IR spectra of pure AZB and $AZB_{0.5}$@MIL-53(Al) (**4**), see the Supporting Information, Figures S2 and S3).

Two bands at 776 and 690 cm^{-1} can be assigned to *trans*-azobenzene.[35] After exposure to UV light, a decrease of their intensities combined with the appearance of two new bands at 759 and 703 cm^{-1} was detected, deriving from a partial conversion of *trans*- to *cis*-azobenzene. Such a successful isomerization process was found in AZB_5@MOF-5 (**1**), $AZB_{0.66}$@MIL-68(In) (**2**), and $AZB_{0.66}$@MIL-68(Ga) (**3**). In a lower ratio and only after longer irradiation times, it was also induced in pure solid azobenzene, in contrast to reports in the literature.[36] From our experiments, we estimated a ratio of *cis*-

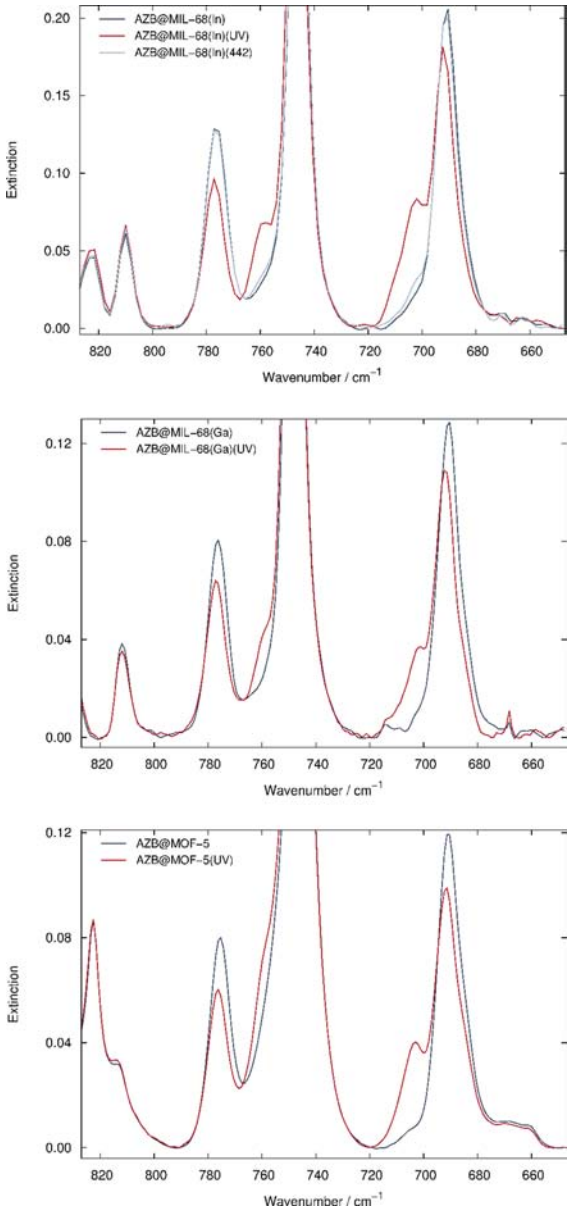

Figure 2. IR spectra of azobenzene (AZB) loaded MOFs before (dark blue) and after (red) irradiation with UV light (λ = 325 nm). For $AZB_{0.66}$@MIL-68(In) (**2**) (top), the IR spectrum after irradiation with λ = 442 nm (light blue) is additionally shown.

azobenzene of 12%. The obtained fraction of *cis*-azobenzene embedded in MOFs depends slightly on the host material at a given irradiation time with a maximum for MIL-68(In). The quantitative analysis of the band areas results in a ratio of 30%/27%/25% *cis*-azobenzene for $AZB_{0.66}$@MIL-68(In) (**2**), $AZB_{0.66}$@MIL-68(Ga) (**3**), and AZB_5@MOF-5 (**1**), respectively.[37] When exposed to light with longer wavelengths (442 nm), the reverse process is induced, resulting in the recovery of almost 100% *trans*-azobenzene, as shown exemplarily for $AZB_{0.66}$@MIL-68(In) (**2**) in Figure 2 (top). Because of a progressing opacity of the KBr pellet, a longer irradiation to gain 100% of the *cis*-isomer was not possible. However, for MIL-53(Al) as host material, no conversion of the embedded *trans*-azobenzene could be achieved using even longer irradiation times or different wavelengths (Supporting Information, Table S1).

dx.doi.org/10.1021/ic302856b | *Inorg. Chem.* 2013, 52, 2744−2749

To understand the different switching behavior of $AZB_{0.5}$@MIL-53(Al) (**4**) and $AZB_{0.66}$@MIL-68(Ga) (**3**) and to characterize the underlying host−guest interactions, the knowledge of their crystal structures and thus the arrangement of the guest molecules within the respective host materials is essential. As all substances are only available as polycrystalline powders after the gas phase loading, the structure solutions had to be carried out from X-ray powder diffraction data. To get the best data possible, high-resolution synchrotron powder diffraction data were recorded at beamline BM01B at the ESRF/Grenoble at low temperatures (120 K) to diminish the motion of the guest molecules within the MOF pores.

The diffraction patterns obtained at room temperature and 120 K were indexed with the programs ITO[26] and FOX.[27] Le Bail fits in Jana2006[28] (Supporting Information, Figures S7, S8, S10−S12) were used to refine the unit cells, zero shifts, and profile parameters. The structures of $AZB_{0.66}$@MIL-68(Ga) (**3**) and $AZB_{0.5}$@MIL-53(Al) (**4**) were finally solved with FOX.[27] The atomic positions of the known crystal structures of MIL-68(Ga)[30] and MIL-53(Al)[29] with the unit cell parameters obtained from the Le Bail fits were used as starting parameters together with the known molecular structure of *trans*-azobenzene.[38] The positions of azobenzene were determined by a global optimization algorithm (parallel tempering) in direct space and refined with the program GSAS.[32] More details are given in the Experimental Section. The crystallographic data are summarized in Table 1.

The crystal structure of $AZB_{0.5}$@MIL-53(Al) (**4**) is shown in Figure 3. As the structure of MIL-53(Al) is well-known,[29,33] the structure description will focus on the arrangement of the guest molecules inside the MIL-53(Al) pores. Compound **4** crystallizes in the orthorhombic space group *Pnma* (No. 62) with four formula units per unit cell, as already found for MIL-53(Al)*as*.[33] AZB occupies the general site 8*d*, but due to steric reasons, a simultaneous occupation of all symmetry-generated positions is not possible. The refinement of the occupancy of all positions of the AZB molecule converged at a value of 0.24, in good agreement with the results of the elemental analysis. As described for other systems,[6] due to dynamic or static disorder over all these positions, no reduction of symmetry is observed. AZB is oriented almost parallel to the one-dimensional channels of the host. The shortest C−C distance between AZB and the host is 3.49 Å (C7−C3x) and the shortest C−N distance is 3.47 Å (N2−C3x). These distances point to weak van der Waals interactions, as also obvious from the space-filling representation in Figure 3 (bottom). Furthermore, the aromatic rings of the AZB guest and the bdc linker of the host are aligned parallel in such a way that $\pi-\pi$ interactions are likely to occur. Assuming that only every fourth AZB position within a channel is occupied, the C−C distances between two AZB molecules start at 3.34 Å (C1−C4) and the shortest C−N distances at 3.48 Å (N2−C6), again in the range of van der Waals interactions. Compared to the room-temperature crystal structure of *trans*-azobenzene,[38] these distances are slightly shorter (C−C: 3.540(2) Å and C−N: 3.622(1) Å). From Figure 3 (bottom), it is obvious that the light-induced isomerization to *cis*-azobenzene is obviously sterically hindered within the channels of MIL-53(Al).

A different picture is found for $AZB_{0.66}$@MIL-68(Ga) (**3**), as shown in Figure 4. AZB molecules are only found within the larger six-membered channels of the host. Two symmetry-independent sites are occupied by AZB molecules, both located on the general position 16*h*. The occupancies of both sites

Table 1. Crystallographic Data and Rietveld Refinements/Le Bail Fits of 1−4 from Synchrotron Powder Diffraction Data

	AZB_5@MOF-5 (**1**)	$AZB_{0.66}$@MIL-68(In) (**2**)		$AZB_{0.66}$@MIL-68(Ga) (**3**)		$AZB_{0.5}$@MIL-53(Al) (**4**)	
T/K	298[a]	298[a]	120[a]	298[a]	120[b]	298[a]	120[b]
space group, Z	*Fm*3*m* (No. 225), 24	*Cmcm* (No. 63), 12	*Pnma* (No. 62), 12	*Cmcm* (No. 63), 12	*Cmcm* (No. 63), 12	*Pnma* (No. 62), 4	*Pnma* (No. 62), 4
a/Å	25.8226(3)	21.8166(5)	37.1635(7)	21.2058(8)	21.120(1)	17.0078(3)	17.2258(3)
b/Å		37.4347(8)	7.21219(9)	36.500(1)	36.617(3)	6.63624(9)	6.6385(1)
c/Å		7.2214(1)	21.7176(4)	6.7413(2)	6.7395(2)	12.4009(2)	12.0690(3)
V/Å^3	17218.6(2)	5897.7(2)	5821.0(2)	5217.9(4)	5212.0(6)	1399.67(4)	1380.13(6)
R_p,wR_p	0.0513/0.0661	0.1125/0.1481	0.0669/0.0862	0.0963/0.1253	0.0960/0.1120	0.1137/0.1605	0.0942/0.1212
R_B					4.77		7.12
GOF[a]/χ^2[b]	1.29	1.47	1.71	1.03	7.931	1.11	3.514
Occ. (AZB)					0.21		0.24

[a]Le Bail fit. [b]Rietveld refinement.

dx.doi.org/10.1021/ic302856b | *Inorg. Chem.* 2013, 52, 2744−2749

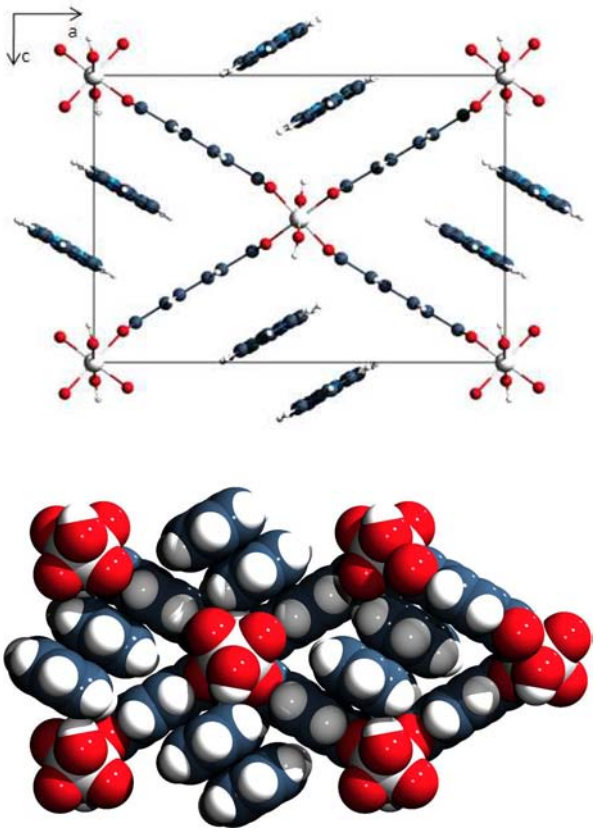

Figure 3. (top) Unit cell of $AZB_{0.5}$@MIL-53(Al) (**4**) with a view along [010]. (bottom) Space-filling representation of **4**. Note: not all symmetry-related AZB positions are shown; each position is occupied with 24%.

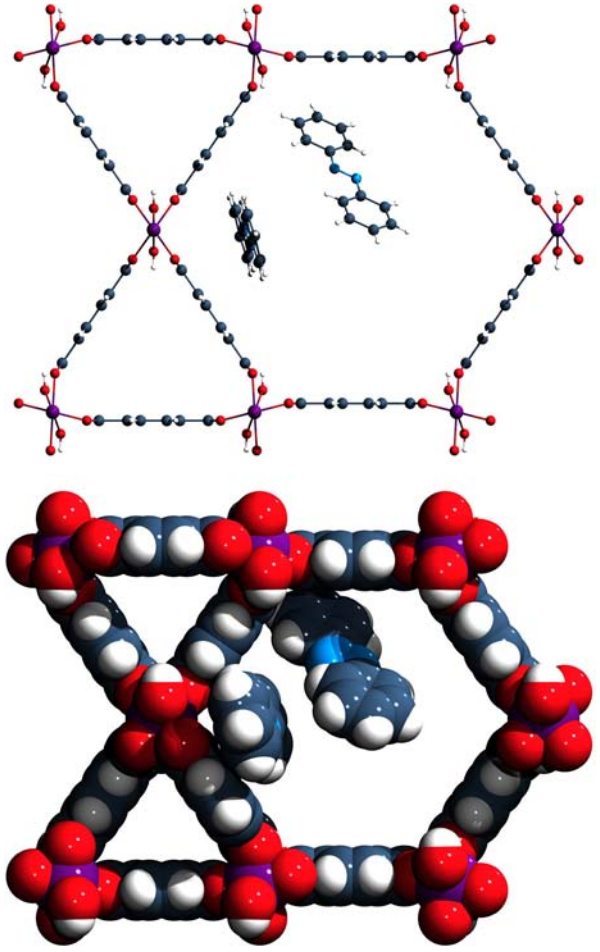

Figure 4. (top) View of the crystal structure of $AZB_{0.66}$@MIL-68(Ga) (**3**) along [001]. (bottom) Space-filling representation of **3**. Note: not all symmetry-related AZB positions are shown; each position is occupied with ~21%.

refined to very similar values (~0.21), again in reasonable agreement with the results of the elemental analysis. Only one AZB is oriented parallel to the one-dimensional channels along [001]; the other AZB is almost perpendicular to the former in the (001) plane. The shortest C−C distance between AZB and the host is 2.99 Å (C20−C9), and the shortest C−N distance is 3.79 Å (N1−C8). These distances are slightly different to those obtained for $AZB_{0.5}$@MIL-53(Al) (**4**), but still in the same range, as expected for van der Waals interactions (see space-filling representation in Figure 4 (bottom)). It cannot be excluded that, for $AZB_{0.66}$@MIL-68(Ga) (**3**) with two symmetry-independent sites for the AZB guests, the uncertainties in determining the guests positions—and such the intermolecular distances—are higher than those obtained for **4**. The standard deviations obtained from the Rietveld analysis surely underestimate these uncertainties. Furthermore, due to the fact that two symmetry-independent positions are only partly occupied, a reasonable assignment of intermolecular AZB distances is not possible. Figure 4 shows unambiguously that, within the larger channels of MIL-68(Ga), the light-induced isomerization to *cis*-azobenzene can occur without any sterical hindrance.

■ CONCLUSION

In conclusion, we have embedded photochromic azobenzene in different MOFs and showed that the *trans*/*cis* isomerization can also occur within the confined channels or pores of these hosts and is even improved compared to that of pure solid azobenzene. However, for MIL-53(Al), no *trans*/*cis* isomerization was found. Crystal structures reveal that the size and the shape of the host's channels, as well as the orientation of azobenzene within these channels, are responsible for this different behavior. Fujita et al. reported porous coordination networks consisting of ZnI_2 and tris(4-pyridyl)triazine, which were loaded with (*Z*)-stilbene via a solution process.[39] The successful inclusion was confirmed by an X-ray single-crystal structure analysis. Irradiation (λ_{ex} = 400−500 nm) of this inclusion compound suspended in a solution resulted in a 98% conversion to (*E*)-stilbene. This inclusion compound can even act as a catalyst for the $Z \rightarrow E$ photoisomerization, but the authors did not report any dependence of the photoisomerization upon sterical hindrance within the pores of the porous coordination network. This aspect of our work seems to be quite new, so we are planning to broaden our studies to further MOFs with different shapes and sizes of the pores as well as to other guests, such as fluorinated and perfluorinated azobenzene.[40] Also, the influence of the concentration of the guest within the host's pores on the optical properties shall be investigated. First results show that MOF-5 can be loaded with lower ratios of guest molecules. Finally, the investigation of XRPD patterns of different AZB@MOF systems under irradiation seems to be worthwhile, as already shown by Kitagawa et al.[25]

dx.doi.org/10.1021/ic302856b | *Inorg. Chem.* 2013, 52, 2744−2749

■ ASSOCIATED CONTENT

Supporting Information

Details of the irradiation experiments, elemental analyses, UV/vis and additional IR spectra, XRPD patterns of loaded and unloaded MOFs, and XRPD patterns with Le Bail and Rietveld fits. This material is available free of charge via the Internet at http://pubs.acs.org.

■ AUTHOR INFORMATION

Corresponding Author

*E-mail: uwe.ruschewitz@uni-koeln.de .

Notes

The authors declare no competing financial interest.

■ ACKNOWLEDGMENTS

D.H. acknowledges the Fonds der Chemischen Industrie for a doctoral stipend. We thank D. Hertel and K. Meerholz for measurements at their IR spectrometer under laser irradiation.

■ REFERENCES

(1) Férey, G. *Chem. Soc. Rev.* **2008**, *37*, 191.
(2) Suh, M. P.; Park, H. J.; Prasad, T. K.; Lim, D.-W. *Chem. Rev.* **2012**, *112*, 782.
(3) Zlotea, C.; Campesi, R.; Cuevas, F.; Leroy, E.; Dibandjo, P.; Volkringer, C.; Loiseau, T.; Férey, G.; Latroche, M. *J. Am. Chem. Soc.* **2010**, *132*, 2991.
(4) Wu, H.; Reali, R. S.; Smith, D. A.; Trachtenberg, M. C.; Li, J. *Chem.—Eur. J.* **2010**, *16*, 13951.
(5) Li, J.-R.; Sculley, J.; Zhou, H.-C. *Chem. Rev.* **2012**, *112*, 869.
(6) Alaerts, L.; Maes, M.; Giebeler, L.; Jacobs, P. A.; Martens, J. A.; Denayer, J. F. M.; Kirschhock, E. E. A.; De Vos, D. E. *J. Am. Chem. Soc.* **2008**, *43*, 14170.
(7) Maes, M.; Vermoortele, F.; Alaerts, L.; Couck, S.; Kirschhock, C. E. A.; Denayer, J. F. M.; De Vos, D. E. *J. Am. Chem. Soc.* **2010**, *132*, 15277.
(8) Lee, J. Y.; Farha, O. K.; Roberts, J.; Scheidt, K. A.; Nguyen, S. T.; Hupp, J. T. *Chem. Soc. Rev.* **2009**, *38*, 1248.
(9) Hermes, S.; Schröter, M.-K.; Schmid, R.; Khodeir, L.; Muhler, M.; Tissler, A.; Fischer, R. W.; Fischer, R. A. *Angew. Chem., Int. Ed.* **2005**, *44*, 6237.
(10) Esken, D.; Turner, S.; Lebedev, O. I.; Van Tendeloo, G.; Fischer, R. A. *Chem. Mater.* **2010**, *22*, 6393.
(11) Horcajada, P.; Serre, C.; Vallet-Regí, M.; Sebban, M.; Taulelle, F.; Férey, G. *Angew. Chem., Int. Ed.* **2006**, *45*, 5974.
(12) Horcajada, P.; Chalati, T.; Serre, C.; Gillet, B.; Sebrie, C.; Baati, T.; Eubank, J. F.; Heurtaux, D.; Clayette, P.; Kreuz, C.; Chang, J.-S.; Hwang, Y. K.; Marsaud, V.; Bories, P.-N.; Cynober, L.; Gil, S.; Férey, G.; Couvreur, P.; Gref, R. *Nat. Mater.* **2010**, *9*, 172.
(13) Seidel, C.; Ruschewitz, U.; Schuy, A.; Woike, T.; Schaniel, D. *Z. Anorg. Allg. Chem.* **2008**, *634*, 2018.
(14) Ruschewitz, U.; Hermann, D. *Z. Anorg. Allg. Chem.* **2010**, *636*, 2068.
(15) Nägele, T.; Hoche, R.; Zinth, W.; Wachtveitl, J. *Chem. Phys. Lett.* **1997**, *272*, 489.
(16) Kojima, M.; Nakajoh, M.; Nebashi, S.; Kurita, N. *Res. Chem. Intermed.* **2004**, *30*, 181.
(17) Modrow, A.; Zargarani, D.; Herges, R.; Stock, N. *Dalton Trans.* **2011**, *40*, 4217.
(18) Bernt, S.; Feyand, M.; Modrow, A.; Wack, J.; Senker, J.; Stock, N. *Eur. J. Inorg. Chem.* **2011**, 5378.
(19) Modrow, A.; Zargarani, D.; Herges, R.; Stock, N. *Dalton Trans.* **2012**, *41*, 8690.
(20) Park, J.; Yuan, D.; Pham, K. T.; Li, J.-R.; Yakovenko, A.; Zhou, H.-C. *J. Am. Chem. Soc.* **2012**, *134*, 99.
(21) Burke, N. J.; Burrows, A. D.; Mahon, M. F.; Warren, J. E. *Cryst. Growth Des.* **2006**, *6*, 546.
(22) Schaate, A.; Dühnen, S.; Platz, G.; Lilienthal, S.; Schneider, A. M.; Behrens, P. *Eur. J. Inorg. Chem.* **2012**, 790.
(23) Hoffmann, K.; Resch-Genger, U.; Marlow, F. *Microporous Mesoporous Mater.* **2000**, *41*, 99.
(24) Abrahams, B. F.; Moylan, M.; Orchard, S. D.; Robson, R. *Angew. Chem., Int. Ed.* **2003**, *42*, 1848.
(25) Yanai, N.; Uemura, T.; Inoue, M.; Matsuda, R.; Fukushima, T.; Tsujimoto, M.; Isoda, S.; Kitagawa, S. *J. Am. Chem. Soc.* **2012**, *134*, 4501.
(26) Visser, J. W. *J. Appl. Crystallogr.* **1969**, *2*, 89.
(27) Favre-Nicolin, V.; Černý, R. *J. Appl. Crystallogr.* **2002**, *35*, 734.
(28) Petríček, V.; Dušek, M.; Palatinus, L. *Jana2006: The crystallographic computing system*; Institute of Physics: Praha, Czech Republic, 2006.
(29) Vougo-Zanda, M.; Huang, J.; Anokhina, E.; Wang, X.; Jacobson, A. J. *Inorg. Chem.* **2008**, *47*, 11535.
(30) Volkringer, C.; Meddouri, M.; Loiseau, T.; Guillou, N.; Marrot, J.; Férey, G.; Haouas, M.; Taulelle, F.; Audebrand, N.; Latroche, M. *Inorg. Chem.* **2008**, *47*, 11892.
(31) Harada, J.; Ogawa, K. *J. Am. Chem. Soc.* **2004**, *126*, 3539.
(32) (a) Larson, A. C.; Von Dreele, R. B. *Los Alamos Laboratory, Report No. LAUR 86-748*; Los Alamos Laboratory: Los Alamos, NM, 1987. (b) Toby, B. H. *J. Appl. Crystallogr.* **2001**, *34*, 210.
(33) Loiseau, T.; Serre, C.; Huguenard, C.; Fink, G.; Taulelle, F.; Henry, M.; Bataille, T.; Férey, G. *Chem.—Eur. J.* **2004**, *10*, 1373.
(34) Li, H.; Eddaoudi, M.; O'Keeffe, M.; Yaghi, O. M. *Nature* **1999**, *402*, 276.
(35) Biswas, N.; Umapathy, S. *J. Phys. Chem. A* **1997**, *101*, 5555.
(36) Tsuda, M.; Kuratani, K. *Bull. Chem. Soc. Jpn.* **1964**, *37*, 1284.
(37) To estimate the *cis*-to-*trans* ratio from the measured IR spectra, the areas of the bands at 776 and 690 cm^{-1} (*trans*-AZB) as well as 777, 759, 703, and 688 cm^{-1} (*cis*-AZB) were determined by fitting the respective peaks with a Voigt function after adjustment of the baseline. The UV/vis measurement of AZB_5@MOF-5 (**1**) without illumination (Figure S1, Supporting Information) shows that the ground state of AZB_5@MOF only contains *trans*-AZB. Accordingly, the areas of the two bands of *trans*-AZB in the not illuminated sample were set to 100%. As two of the four bands of *cis*-AZB overlap with those of *trans*-AZB, the areas of underlying *cis*-AZB bands were calculated from the areas of the two nonoverlapping bands at 759 and 703 cm^{-1}. The relative band intensities of *cis*-AZB were taken from the literature (ref 41). For $AZB_{0.66}$@MIL-68(In) (**2**) and $AZB_{0.66}$@MIL-68(Ga) (**3**), a similar procedure was applied, as the nonilluminated compounds only contain *trans*-AZB as proven by IR spectroscopy
(38) Harada, J.; Ogawa, K. *J. Am. Chem. Soc.* **2004**, *126*, 3539.
(39) Ohara, K.; Inokuma, Y.; Fujita, M. *Angew. Chem., Int. Ed.* **2010**, *49*, 5507.
(40) Ruschewitz, U.; Hermann, D. *Z. Anorg. Allg. Chem.* **2012**, *638*, 1574.
(41) Fiegl, H.; Köhn, A.; Hättig, C.; Ahlrichs, R. *J. Am. Chem. Soc.* **2003**, *125*, 9821.